

## External and Internal Guest Binding of a Highly Charged Supramolecular Host in Water: Deconvoluting the Very Different Thermodynamics

Carmelo Sgarlata,<sup>†</sup> Jeffrey S. Mugridge,<sup>†</sup> Michael D. Pluth,<sup>†</sup>  
 Bryan E. F. Tiedemann,<sup>†</sup> Valeria Zito,<sup>‡</sup> Giuseppe Arena,<sup>\*,§</sup> and  
 Kenneth N. Raymond<sup>\*,†</sup>

*Department of Chemistry, University of California, Berkeley and Chemical Science Division, Lawrence Berkeley National Laboratory, Berkeley, California 94720-1460, Istituto di Biostrutture e Bioimmagini, CNR, Viale Andrea Doria 6, 95125 Catania, Italy, and Dipartimento di Scienze Chimiche, Università degli Studi di Catania, Viale Andrea Doria 6, 95125 Catania, Italy*

Received July 9, 2009; E-mail: raymond@socrates.berkeley.edu; garena@unict.it

**Abstract:** NMR, UV–vis, and isothermal titration calorimetry (ITC) measurements probe different aspects of competing host–guest equilibria as simple alkylammonium guest molecules interact with both the exterior (ion-association) and interior (encapsulation) of the [Ga<sub>4</sub>L<sub>6</sub>]<sup>12-</sup> supramolecular assembly in water. Data obtained by each independent technique measure different components of the host–guest equilibria and only when analyzed together does a complete picture of the solution thermodynamics emerge. Striking differences between the internal and external guest binding are found. External binding is enthalpy driven and mainly due to attractive interactions between the guests and the exterior surface of the assembly while encapsulation is entropy driven as a result of desolvation and release of solvent molecules from the host cavity.

### Introduction

Guest binding is a crucial property for the role of supramolecular catalysis. Supramolecular assemblies<sup>1–5</sup> can interact with multiple guests simultaneously, and the driving forces for guest binding can include both specific interactions between the guest and host functional groups,<sup>6</sup> as well as nonspecific, weak, supramolecular interactions such as CH– $\pi$ ,  $\pi$ – $\pi$ , or cation– $\pi$  interactions.<sup>7–10</sup> Solvent also frequently plays a critical role in

molecular recognition: displacement of solvent molecules from a host cavity and guest desolvation must typically occur before encapsulation can take place.<sup>11</sup> All of these driving forces can generate different enthalpic and entropic contributions to the free energy of guest binding, making the determination of thermodynamic parameters for host–guest equilibria complicated and difficult. Such parameters have been measured by solution NMR and UV–vis spectroscopy, but each of these methods has inherent limitations due to their different time scales and observables. NMR and UV–vis equilibrium measurements can be used to indirectly determine enthalpy and entropy values as a function of temperature, but this makes these two values statistically correlated<sup>12</sup> and inaccurate if there is a significant change in heat capacity during the reaction.<sup>13</sup> Isothermal titration calorimetry (ITC) enables direct measurement of the heat change induced by guest binding at a constant temperature and can provide useful information about the nature of host–guest

<sup>†</sup> University of California and Lawrence Berkeley National Laboratory.

<sup>‡</sup> Istituto di Biostrutture e Bioimmagini, CNR.

<sup>§</sup> Università degli Studi di Catania.

- (1) (a) Yoshizawa, M.; Klosterman, J. K.; Fujita, M. *Angew. Chem., Int. Ed.* **2009**, *48*, 3418–3438. (b) Dalgarno, S. J.; Power, N. P.; Atwood, J. L. *Coord. Chem. Rev.* **2008**, *252*, 825–841. (c) Tranchemontagne, D. J.; Ni, Z.; O’Keeffe, M.; Yaghi, O. M. *Angew. Chem., Int. Ed.* **2008**, *47*, 5136–5147. (d) Oshovsky, G. V.; Reinhoudt, D. N.; Verboom, W. *Angew. Chem., Int. Ed.* **2007**, *46*, 2366–2393. (e) Ward, M. *Chem. Commun.* **2009**, *30*, 4487–4499.
- (2) (a) Leininger, S.; Olenyuk, B.; Stang, P. J. *Chem. Rev.* **2000**, *100*, 853–908. (b) Northrop, B. H.; Zheng, Y.-R.; Chi, K.-W.; Stang, P. J. *Acc. Chem. Res.* **2009**, *42*, 1554–1563.
- (3) (a) Vriezema, D. M.; Aragones, M. C.; Elemans, J.; Cornelissen, J.; Rowan, A. E.; Nolte, R. J. M. *Chem. Rev.* **2005**, *105*, 1445–1489. (b) Ariga, K.; Hill, J. P.; Lee, M. V.; Vinu, A.; Charvet, R.; Acharya, S. *Sci. Technol. Adv. Mater.* **2008**, *9*, 014109. (c) Koblenz, T. S.; Wassenaar, J.; Reek, J. N. H. *Chem. Soc. Rev.* **2008**, *37*, 247–262.
- (4) (a) Fujita, M.; Tomimaga, M.; Hori, A.; Therrien, B. *Acc. Chem. Res.* **2006**, *39*, 371–380. (b) Yoshizawa, M.; Tamura, M.; Fujita, M. *Science* **2006**, *312*, 251–254. (c) Suzuki, K.; Iida, J.; Sato, S.; Kawano, M.; Fujita, M. *Angew. Chem., Int. Ed.* **2008**, *47*, 5780–5782.
- (5) (a) Kang, J.; Rebek, J., Jr. *Nature* **1997**, *385*, 50–52. (b) L. Trembleau, L.; Rebek, J., Jr. *Science* **2003**, *301*, 1219–1220. (c) Ajami, D.; Rebek, J., Jr. *Proc. Natl. Acad. Sci. U.S.A.* **2007**, *104*, 16000–16003.
- (6) Iwasawa, T.; Hooley, R. J.; Rebek, J., Jr. *Science* **2007**, *317*, 493–496.

- (7) Williams, D. H.; Westwell, M. S. *Chem. Soc. Rev.* **1998**, *27*, 57–64.
- (8) Meyer, E. A.; Castellano, R. K.; Diederich, F. *Angew. Chem., Int. Ed.* **2003**, *42*, 1210–1250.
- (9) Ma, J. C.; Dougherty, D. A. *Chem. Rev.* **1997**, *97*, 1303–1324.
- (10) Nishio, M. *Tetrahedron* **2005**, *61*, 6923–6950.
- (11) Klotz, I. M. *Ligand-Receptor Energetics*; John Wiley & Sons: New York, 1997.
- (12) (a) Leung, D. H.; Bergman, R. G.; Raymond, K. N. *J. Am. Chem. Soc.* **2008**, *130*, 2798–2805. (b) Inoue, Y.; Wada, T. In *Advances in Supramolecular Chemistry*; Gokel, G. W., Ed.; JAI Press: Greenwich, CT, 1997; Volume 4, pp 55–96. (c) Sharp, K. *Protein Sci.* **2001**, *10*, 661–667.
- (13) (a) Horn, J. R.; Russell, D.; Lewis, E. A.; Murphy, K. P. *Biochemistry* **2001**, *40*, 1774–1778. (b) Horn, J. R.; Brandts, J. F.; Murphy, K. P. *Biochemistry* **2002**, *41*, 7501–7507. (c) Naghibi, H.; Tamura, A.; Sturtevant, J. M. *Proc. Natl. Acad. Sci. U.S.A.* **1995**, *92*, 5597–5599.

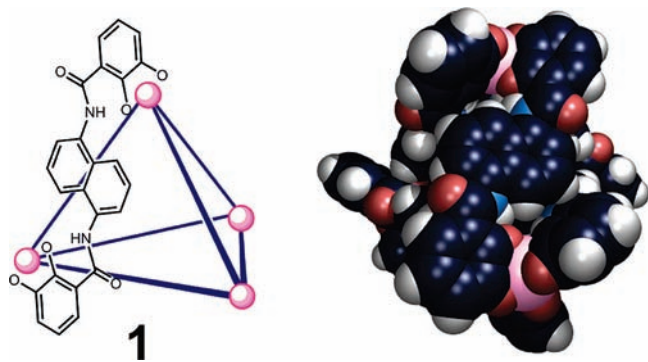


**Figure 1.** Schematic of the  $[\text{Ga}_4\text{L}_6]^{12-}$  framework, only one ligand is shown for clarity (left). Space-filling model of **1** as viewed down the two-fold axis (right).

interactions.<sup>14</sup> This study uses the complementary techniques of NMR, UV–vis, and ITC to untangle the thermodynamics ( $\Delta G^\circ$ ,  $\Delta H^\circ$ , and  $\Delta S^\circ$ ) of sequential internal and external guest binding to a highly charged supramolecular host.

We have reported a series of self-assembling, tetrahedral  $[\text{M}_4\text{L}_6]^{n-}$  ( $\text{L} = 1,5\text{-bis}(2,3\text{-dihydroxybenzamido})\text{naphthalene}$ ) supramolecular assemblies<sup>15</sup> that act as chiral, nanoscale flasks for encapsulated guest catalysts or transient guest substrates and can carry out enzyme-like chemical transformations.<sup>16–18</sup> The  $[\text{Ga}_4\text{L}_6]^{12-}$  assembly (Figure 1, **1**) has received the most attention and is used exclusively in the present study. The hydrophobic interior cavity of **1** can encapsulate a variety of hydrophobic monocationic<sup>19</sup> and neutral guest molecules.<sup>20</sup> The highly anionic exterior surface of **1** imparts solubility in water and other polar solvents, as well as an affinity for external ion-association of cationic molecules (Figure 2a); indirect observation of external ion-association has previously been observed in kinetic studies,<sup>21,22</sup> diffusion-based  $^1\text{H}$  NMR experiments,<sup>23</sup> as well as solid-state structures.<sup>24</sup> The species distribution of these competing interior and exterior host–guest equilibria (Figure 2b), which cannot be deconvoluted by NMR, UV–vis, or ITC alone, here has been elucidated by analyzing together the different observables measured by each technique.

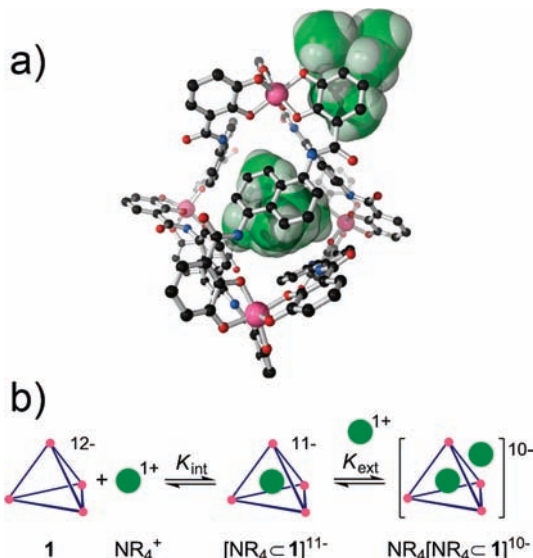


**Figure 2.** (a) Internally and externally bound  $\text{NEt}_4^+$  to **1**, adapted from the crystal structure of  $\text{K}_5(\text{NEt}_4)_6[\text{NEt}_4 \subset \text{Fe}_4\text{L}_6]$ .<sup>15</sup> (b) Schematic equilibria for internal ( $K_{\text{int}}$ ) and external ( $K_{\text{ext}}$ )  $\text{NEt}_4^+$  guest binding with **1**. The symbol  $\subset$  denotes encapsulation.

## Experimental Section

**General Synthetic Procedures.**  $\text{K}_{12}[\mathbf{1}]$  was prepared as previously described<sup>15</sup> and stored under nitrogen. Ammonium salts  $\text{NEt}_4\text{Cl}$  and  $\text{NMe}_4\text{Cl}$  were purchased from Sigma-Aldrich and recrystallized from ethanol prior to use. All solvents were degassed with nitrogen prior to use.

**Isothermal Titration Calorimetry (ITC).** Data for determination of the thermodynamic parameters were obtained using a nanoisothermal titration calorimeter (Nano-ITC III CSC 5300) at 25 °C in water with 0.1 M KCl. Since accurate determination of the enthalpy of reaction requires concentrations to be precisely known, the effective molecular weight of  $\text{K}_{12}[\mathbf{1}]$  was determined via thermogravimetric analysis (TGA, Figure S1, Supporting Information (SI)). The first decrease observed in the TGA curve (up to 130 °C) accounts for the adsorbed residual solvent that amounts to 5–8% of the total host weight. The final weight % at 800 °C is consistent with the expected value based on the inorganic components (potassium and gallium oxides) of the host. The concentration of the hygroscopic  $\text{NEt}_4\text{Cl}$  and  $\text{NMe}_4\text{Cl}$  was obtained indirectly by determining the chloride concentration according to the Mohr procedure.<sup>25</sup>

ITC measurements were carried out by titration of an aqueous guest solution (in 0.1 M KCl) into a 1 mM host solution (in 0.1 M KCl).  $^1\text{H}$  NMR studies have previously shown that the encapsulation process can be relatively slow.<sup>26</sup> As such, preliminary ITC experiments were run with different time intervals between guest addition, ranging from 300 to 1200 s; complete equilibration of the guest encapsulation process was achieved only at the longer time intervals. Accordingly, the time interval between each of the first 8–9 additions was set at 1200 s. Six and twelve independent ITC experiments were run to explore the 0.2–0.8 equiv and the 0.2–20 equiv regime, respectively. These experiments totaled 120 and 300 points, respectively. The heats of dilution were determined in separate experiments by titration of the solution of the guest (in 0.1 M KCl) into a solution containing 0.1 M KCl. The net heat

- (14) Schmidtchen, F. P. In *Analytical Methods in Supramolecular Chemistry*; Schalley, C., Ed.; Wiley-VCH Verlag: Weinheim, 2007; pp 55–78.
- (15) Caulder, D. L.; Powers, R. E.; Parac, T. N.; Raymond, K. N. *Angew. Chem., Int. Ed.* **1998**, *37*, 1840–1843.
- (16) Fiedler, D.; Leung, D. H.; Bergman, R. G.; Raymond, K. N. *Acc. Chem. Res.* **2005**, *38*, 349–358.
- (17) (a) Pluth, M. D.; Bergman, R. G.; Raymond, K. N. *Science* **2007**, *316*, 85–88. (b) Pluth, M. D.; Fiedler, D.; Mugridge, J. S.; Bergman, R. G.; Raymond, K. N. *Proc. Natl. Acad. Sci. U.S.A.* **2009**, *106*, 10438–10443.
- (18) Pluth, M. D.; Bergman, R. G.; Raymond, K. N. *Acc. Chem. Res.* **2009**, *42*, 1650–1659.
- (19) Parac, T. N.; Caulder, D. L.; Raymond, K. N. *J. Am. Chem. Soc.* **1998**, *120*, 8003–8004.
- (20) (a) Biros, S. M.; Bergman, R. G.; Raymond, K. N. *J. Am. Chem. Soc.* **2007**, *129*, 12094–12095. (b) Hastings, C. J.; Pluth, M. D.; Biros, S. M.; Bergman, R. G.; Raymond, K. N. *Tetrahedron* **2008**, *64*, 8362–8367.
- (21) Leung, D. H.; Bergman, R. G.; Raymond, K. N. *J. Am. Chem. Soc.* **2006**, *128*, 9781–9797.
- (22) Fiedler, D.; van Halbeek, H.; Bergman, R. G.; Raymond, K. N. *J. Am. Chem. Soc.* **2006**, *128*, 10240–10252.
- (23) Pluth, M. D.; Tiedemann, B. E. F.; van Halbeek, H.; Nunlist, R.; Raymond, K. N. *Inorg. Chem.* **2008**, *47*, 1411–1413.
- (24) Pluth, M. D.; Johnson, D. W.; Szigethy, G. S.; Davis, A. V.; Teat, S. J.; Oliver, A. G.; Bergman, R. G.; Raymond, K. N. *Inorg. Chem.* **2009**, *48*, 111–120.

- (25) Kolthoff, I. M.; Sandell, E. B.; Meehan, E. J.; Bruckenstein, S. *Quantitative Chemical Analysis*; The Macmillan Company: New York, 1969; Vol. 2.
- (26) (a) Davis, A. V.; Raymond, K. N. *J. Am. Chem. Soc.* **2005**, *127*, 7912–7919. (b) Davis, A. V.; Fiedler, D.; Seeber, G.; Zahl, A.; van Eldik, R.; Raymond, K. N. *J. Am. Chem. Soc.* **2006**, *128*, 1324–1333.

obtained was fit using two different computer programs: Hyper $\Delta H^{27}$  and BindWorks (TA Instruments, New Castle, DE). Hyper $\Delta H$  allows for the simultaneous fitting of data from multiple titrations. The results obtained with both software packages are consistent with one another, and fits for a typical ITC titration are shown in Figure S2, SI.

**UV–Vis Titrations.** Spectrophotometric measurements (Agilent 8453 diode-array spectrophotometer) were carried out at 25 °C in aqueous 0.1 M KCl. Increasing amounts of the guest were added with a precision buret (Hamilton, 1.00 mL) into the measuring cell containing a host solution having the same concentration investigated via ITC. The solution was allowed to fully equilibrate before absorbance values were recorded. Equilibration and data reading and storage were controlled with homemade software. For each independent titration run, 30–40 scans were recorded. Four independent runs were collected for the  $\text{NEt}_4^+ \text{--} \mathbf{1}$  system exploring the 435–800 nm range which leads to a total of more than 50000 absorbance vs volume data points. Typical absorbance changes in the visible region resulting from the addition of  $\text{NEt}_4^+$  to a solution of  $\mathbf{1}$  are shown in Figure S3, SI. Data, corrected for dilution, were analyzed with two different software packages (Specfit<sup>28</sup> and Hyperquad<sup>29</sup>) that make use of a multiwavelength and multivariate treatment of spectral data but use different data-fitting algorithms. Hyperquad is also able to refine data from multiple titrations. The fit for a typical UV–vis titration is reported in Figure S4, SI.

**$^1\text{H}$  NMR Titrations.** NMR titrations were performed by combining the guest and host  $\mathbf{1}$  in varying ratios (0–20 equiv. guest) in separate NMR tubes with 0.1 M KCl in  $\text{D}_2\text{O}$ . The NMR tubes were prepared under nitrogen and allowed to equilibrate overnight. All  $^1\text{H}$  NMR spectra were acquired on a Bruker AV-500 NMR spectrometer with an inverse TBI probe. The chemical shifts corresponding to the  $\text{CH}_2$  and  $\text{CH}_3$  protons of exteriorly bound  $\text{NEt}_4^+$  were simultaneously fit using HyperNMR<sup>30</sup> in the 2–20 equiv guest regime to yield the external binding constant  $K_{\text{ext}}$ . A typical fit obtained with HyperNMR is shown in Figure S5, SI. Attempts to analogously evaluate the  $K_{\text{int}}$  value using the chemical shifts of encapsulated  $\text{NEt}_4^+$  between 0 and 1 equiv of added guest failed due to negligible changes in the chemical shifts of these resonances.

## Result and Discussion

The encapsulation equilibrium ( $K_{\text{int}}$ ) of the strongly binding guest  $\text{NEt}_4^+$  with  $\mathbf{1}$  was first examined (Figure 2b). Due to slow exchange between interior and exterior guest on the NMR time scale, NMR experiments clearly show that the internal binding affinity of  $\text{NEt}_4^+$  is large and the first equivalent of added  $\text{NEt}_4^+$  is exclusively bound to the host interior. Therefore, examination of guest binding equilibria below 1 equiv of  $\text{NEt}_4^+$  allows almost complete isolation of the interior encapsulation equilibrium from exterior guest binding. ITC experiments were accordingly carried out by titrating  $\text{NEt}_4^+$  (0.2–0.8 equiv)<sup>31</sup> into an aqueous solution of  $\mathbf{1}$  (1.0 mM in 0.1 M KCl) while monitoring the heat evolved.<sup>32</sup> The interior binding constant of  $\text{NEt}_4^+$  as determined by ITC is  $\log(K_{\text{int}}) = 4.4(7)$ , which is consistent with previous  $^1\text{H}$  NMR experiments ( $\log(K_{\text{int}}) = 4.55$ ).<sup>26b</sup>

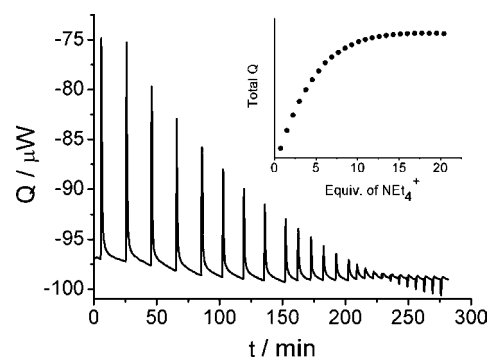


**Figure 3.** ITC data for the addition of a 90 mM solution of  $\text{NEt}_4^+$  into a 1 mM solution of  $\mathbf{1}$ . Inset: total heat vs equiv of  $\text{NEt}_4^+$ .

The exterior binding ( $K_{\text{ext}}$ ) of  $\text{NEt}_4^+$  to  $\mathbf{1}$  was explored using NMR, UV–vis, and ITC experiments. The  $^1\text{H}$  NMR chemical shifts corresponding to the unencapsulated  $\text{NEt}_4^+$  resonances were monitored as a function of added guest (2–20 equiv relative to  $\mathbf{1}$ ). The observed chemical shifts of the unencapsulated guest are the average of the external ion-associated and nonassociated species, due to rapid exchange of these species on the NMR time scale. Chemical shift changes are observed upon exterior association of  $\text{NEt}_4^+$  to  $\mathbf{1}$ , and these can be accurately fit to afford an external binding affinity of  $\log(K_{\text{ext}}) = 1.8(1)$ .<sup>33</sup> Here again, due to the large interior binding constant of  $\text{NEt}_4^+$  in  $\mathbf{1}$ , the observed equilibria past 1 equiv of added  $\text{NEt}_4^+$  correspond almost exclusively to external host–guest interactions.<sup>34</sup>

We also examined UV–vis spectroscopy of the host–guest complex under the same conditions. External host–guest interactions<sup>35</sup> induce small red-shifts of the host charge transfer bands in the visible region of the spectrum (Figure S3, SI).<sup>36</sup> These signals have been accurately analyzed with two different software packages which use factor (multiwavelength) analysis of all the spectrophotometric data.<sup>37</sup> Both clearly showed that the spectral changes were ascribable to one absorbing complex species only ( $\text{NEt}_4[\text{NEt}_4\text{C}\mathbf{1}]^{10-}$ ) and gave a binding affinity of  $\log(K_{\text{ext}}) = 2.04(1)$ . Analogous ITC experiments (Figure 3) afforded a similar value for external guest association of  $\log(K_{\text{ext}}) = 1.96(5)$ , which is consistent with the external binding affinities determined by both  $^1\text{H}$  NMR and UV–vis. Despite the small changes observed in both the NMR and UV–vis spectra, the combination of these with ITC observations provides a clear picture of guest external association.

The binding affinities and thermodynamic parameters obtained by NMR, ITC, and UV–vis for internal and external equilibria (Figure 2b) with  $\text{NEt}_4^+$  are summarized in Table 1.

(27) Gans, P.; Sabatini, A.; Vacca, A. *J. Solution Chem.* **2008**, *37*, 467–476.

(28) Gamp, H.; Maeder, M.; Meyer, C. J.; Zuberbühler, A. D. *Talanta* **1985**, *32*, 95–101.

(29) Gans, P.; Sabatini, A.; Vacca, A. *Talanta* **1996**, *43*, 1739–1753.

(30) Frassinetti, C.; Alderighi, L.; Gans, P.; Sabatini, A.; Vacca, A.; Ghelli, S. *Anal. Bioanal. Chem.* **2003**, *376*, 1041–1052.

(31) In these titrations, the initial data points in the 0.1–0.2 region were excluded due to possible host templation, which is currently under investigation.

(32) (a) Arena, G.; Casnati, A.; Contino, A.; Lombardo, G. G.; Sciotto, D.; Ungaro, R. *Chem.–Eur. J.* **1999**, *5*, 738–744. (b) Arena, G.; Casnati, A.; Contino, A.; Magri, A.; Sansone, F.; Sciotto, D.; Ungaro, R. *Org. Biomol. Chem.* **2006**, *4*, 243–249.

(33) The observed chemical shift changes are modest, but since the exterior guest resonances are sharp, their chemical shifts can be precisely measured and accurately fit.

(34) To further explore these exterior binding interactions, we carried out similar experiments with  $\text{NBut}_4^+$  which, due to its larger size, cannot be encapsulated. However, because  $\text{NBut}_4^+$  is both more hydrophobic and more strongly bound to the host exterior than  $\text{NEt}_4^+$ , this results in precipitation of the host–guest complex after about 6 equiv of guest is added.

(35) Since encapsulation is complete within the first 2–3 points of the vis titration, only the exterior binding was monitored here.

(36) Catechol and naphthalene absorbance bands in the UV region do not change upon guest addition.

(37) (a) Arena, G.; Contino, A.; Longo, E.; Sciotto, D.; Sgarlata, C.; Spoto, G. *Tetrahedron Lett.* **2003**, *44*, 5415–5418. (b) Arena, G.; Contino, A.; Maccarrone, G.; Sciotto, D.; Sgarlata, C. *Tetrahedron Lett.* **2007**, *48*, 8274–8276.

**Table 1.** Thermodynamic Parameters for Interior ( $K_{\text{int}}$ ) and Exterior ( $K_{\text{ext}}$ ) Binding of  $\text{NEt}_4^+$  with  $[\text{Ga}_4\text{L}_6]^{12-}$  (**1**) at 25 °C in Water (0.1 M KCl)<sup>a</sup>

reaction	log K			$\Delta H^\circ$ (kJ mol <sup>-1</sup> )	$\Delta S^\circ$ (J deg <sup>-1</sup> mol <sup>-1</sup> )
	NMR	UV-vis	ITC		
$\text{NEt}_4^+ + \mathbf{1} \xrightleftharpoons{K_{\text{int}}} [\text{NEt}_4 \subset \mathbf{1}]^{11-}$	4.55(6)	n.d.	4.4(7)	-4.1(8)	70(10)
$\text{NEt}_4^+ + [\text{NEt}_4 \subset \mathbf{1}]^{11-} \xrightleftharpoons{K_{\text{ext}}} \text{NEt}_4[\text{NEt}_4 \subset \mathbf{1}]^{10-}$	1.8(1)	2.04(1)	1.96(5)	-27.6(1)	-56(3)

<sup>a</sup>  $\Delta H^\circ$  and  $\Delta S^\circ$  values were calculated by holding  $\log(K_{\text{int}}) = 4.4$  constant, as determined by <sup>1</sup>H NMR and ITC measurements.

These data show that the encapsulation of  $\text{NEt}_4^+$  into **1** is an entropically driven process. Desolvation of the cationic guest and release of solvent from the interior of the empty host assembly account for the large entropic gain observed in this process.<sup>38</sup> Here “empty” refers to the host cavity with no encapsulated guest, which is presumably occupied instead by solvent molecules. Previously measured cavity volumes (~250 Å<sup>3</sup>) suggest 8–10 water molecules can occupy the host interior.<sup>24</sup> The weight loss observed in TGA is consistent with this estimate of the number of encapsulated solvent molecules. Despite the enthalpic cost of host and guest desolvation, the overall encapsulation equilibrium is an enthalpically favored process. We attribute this enthalpic gain to a combination of the highly exothermic association of the positively charged guest to the “empty” 12<sup>-</sup> host (similar to the  $K_{\text{ext}}$  step of Figure 2b and Table 1) and the endothermic encapsulation (due to desolvation) of that ion-associated  $\text{NEt}_4^+$  into the host cavity.

In marked contrast, exterior association of  $\text{NEt}_4^+$  is an enthalpically driven, but entropically disfavored, process. The exothermic external association of  $\text{NEt}_4^+$  is attributed to enthalpically favorable attractive forces, including Coulombic, cation- $\pi$  and CH- $\pi$ , between the guest and the aromatic host exterior. These attractive interactions have been previously observed in solid-state crystallographic<sup>24</sup> and diffusion NMR studies.<sup>23</sup> The diffusion NMR experiments also demonstrated that external association of  $\text{NEt}_4^+$  is favored over  $\text{K}^+$ , used in this study to keep the ionic strength constant.<sup>39</sup> The higher cost for the desolvation of the  $\text{K}^+$  cation also accounts for the preferential exterior association of the  $\text{NEt}_4^+$  species. Furthermore, control ITC experiments carried out in the absence of KCl resulted in a similar amount of heat released as when titrations were performed in the presence of 0.1 M KCl. Values of  $K$ ,  $\Delta H^\circ$ , and  $\Delta S^\circ$  obtained from data collected in the absence of KCl are the same as those reported in Table 1; this rules out any possible effect of KCl on the binding of the investigated guests with **1**.

Since external association is highly exothermic and requires only partial desolvation of the  $\text{NEt}_4^+$  cation, the overall process is observed to be entropically disfavored. Both encapsulation

and ion-association involve a loss of degrees of freedom upon internal or external binding. However, in the case of encapsulation, the loss of degrees of freedom (negative entropy) is more than compensated by the desolvation of the guest and release of solvent (entropy gain) from the “empty” (i.e., solvent filled) host cavity, resulting in a process with an overall positive entropy. For external binding, only partial desolvation of the guest is required, and this does not counterbalance the loss of degrees of freedom, resulting in an overall negative entropy change for this step. This is commonly observed for enthalpically driven host-guest interactions.<sup>32,40–42</sup> Preliminary NMR experiments have also shown the presence of higher-order, externally associated, guest-host stoichiometries with formation constants that are lower than that of the first association, as expected for a host with decreasing charge and some occupied external binding sites.

Internal and external binding interactions of the smaller guest,  $\text{NMe}_4^+$ , with **1** were also investigated. Since  $\text{NMe}_4^+$  is both weakly bound and rapidly exchanging, a direct determination of the internal and external binding affinities with **1** is difficult. In order to isolate the exterior guest binding equilibrium in this system, NMR experiments were carried out in which  $\text{NMe}_4^+$  was titrated into a solution of  $[\text{NEt}_4 \subset \mathbf{1}]^{11-}$  so that the interior cavity is blocked by the strongly bound guest  $\text{NEt}_4^+$ . Fitting the <sup>1</sup>H NMR chemical shifts corresponding to external  $\text{NMe}_4^+$  gives an external binding affinity of  $\log(K_{\text{ext}}) \approx 1$ . Combining these NMR data with preliminary ITC experiments allowed for separation of exterior and interior binding equilibria and showed that  $\text{NMe}_4^+$  is weakly bound to both the host exterior and interior ( $\log(K_{\text{int}}) \approx 2$ ). This is consistent with previous experiments<sup>15</sup> in which  $\text{NEt}_4^+$  readily displaces encapsulated  $\text{NMe}_4^+$  from the cavity of **1**.

## Conclusion

We have used a combination of NMR, UV-vis, and isothermal titration calorimetry to definitively separate and evaluate multiple-guest binding to the interior and exterior of this highly charged supramolecular assembly. There are dramatic differences between the internal and external binding events of the simple alkylammonium cations,  $\text{NEt}_4^+$  and  $\text{NMe}_4^+$ . Encapsulation of  $\text{NEt}_4^+$  into **1** is entropically driven, while external ion-association is enthalpically driven; the encapsulation requires guest desolvation while releasing many solvent molecules, whereas the external association involves ion-association and

(38) (a) Kang, J.; Rebek, J., Jr. *Nature* **1996**, *382*, 239–241. (b) Meissner, R.; Garcias, X.; Mecozzi, S.; Rebek, J., Jr. *J. Am. Chem. Soc.* **1997**, *119*, 77–85. (c) Hooley, R. J.; Van Anda, H. J.; Rebek, J., Jr. *J. Am. Chem. Soc.* **2007**, *129*, 13464–13473. (d) Iwamoto, H.; Mizutani, T.; Kano, K. *Chem., Asian J.* **2007**, *2*, 1267–1275. (e) Zhu, J.; Smithrud, D. B. *Org. Biomol. Chem.* **2007**, *5*, 2992–2999.

(39) The exterior interactions between  $\text{NEt}_4^+$  and **1** cannot be exclusively attributed to simple Coulombic attractions since  $\text{K}^+$  would show similar, if not larger, electrostatic attractive forces toward the anionic exterior of the host. If  $\text{NEt}_4^+$  binding were due to Coulombic attraction only, a large excess of KCl would remove any interaction with **1**; this was clearly not the case, and additional attractive forces have to be involved.

(40) Smithrud, D. B.; Wyman, T. B.; Diederich, F. *J. Am. Chem. Soc.* **1991**, *113*, 5420–5426.

(41) Stauffer, D. A.; Barrans, R. E., Jr.; Dougherty, D. A. *J. Org. Chem.* **1990**, *55*, 2762–2767.

(42) Arena, G.; Casnati, A.; Contino, A.; Gulino, F. G.; Sciotto, D.; Ungaro, R. *J. Chem. Soc., Perkin Trans. 2* **2000**, 419–423.

loss of degrees of freedom. The binding affinities determined by all three techniques are in good agreement with one another and show that  $\text{NEt}_4^+$  binds more strongly to both the host interior and exterior than does  $\text{NMe}_4^+$ . This study illuminates, and for the first time quantifies, the very different internal and external host–guest interactions of the  $[\text{Ga}_4\text{L}_6]^{12-}$  assembly that are a consequence of its high charge and hydrophilic outer space in contrast to its hydrophobic inner space.

**Acknowledgment.** This work has been supported by the Director, Office of Science, Office of Basic Energy Sciences, and the Division of Chemical Sciences, Geosciences, and Biosciences

of the U.S. Department of Energy at LBNL under Contract No. DE-AC02-05CH11231, NSF predoctoral fellowships to J.S.M. and M.D.P., MIUR and Università degli Studi di Catania (Scuola Superiore di Catania and Progetto d'Ateneo). We thank Prof. Robert Bergman for his continuing collaboration.

**Supporting Information Available:** Thermogravimetric analysis, UV–vis spectra, and fits of ITC, UV–vis, and NMR titration data. This material is available free of charge via the Internet at <http://pubs.acs.org>.

JA9056739